

cooling events. The minor low-latitude surface water temperature falls were essentially offset by northward movement of the region.

20. J. F. Marshall and P. J. Davies, *Bur. Miner. Resour. J. Aust. Geol. Geophys.* 3, 85 (1978).

21. We thank our colleagues in the Bureau of Mineral Resources who contributed to discussions on this paper.

22 June 1987; accepted 27 October 1987

Quantitative Three-Dimensional Optical Tomographic Imaging of Supersonic Flows

GREGORY W. FARIS* AND ROBERT L. BYER

Three-dimensional imaging of the density of nitrogen in a supersonic expansion from a nozzle by means of beam-deflection optical tomography is described. With a very simple apparatus, images could be obtained with high absolute accuracy, high spatial resolution, and wide dynamic range.

OPTICAL DIAGNOSTIC TECHNIQUES are useful for making measurements in many transparent systems, including fluid flows, flames, plasmas, and the atmosphere. Optical techniques are nonintrusive and allow fast measurements. However, accurate spatially resolved measurements of real physical parameters are difficult to obtain with optical techniques. Measurement techniques that involve multiple-photon processes and scattering, such as coherent anti-Stokes Raman spectroscopy (CARS) (1), fluorescence imaging (2), Rayleigh scattering (3), and Mie scattering (4), can give spatially resolved measurements but do not easily yield quantitative images. Measurements of optical phase (by means of interferometry, holography, or beam-deflection techniques, for example) or absorption are more direct. These correspond to the measurement of the real or imaginary part of the index of refraction, respectively. However, these techniques give values that are integrated along the line of sight. With tomographic techniques (5), multiple views of integrated measurements through a flow field may be used to reconstruct spatially resolved values of a physical quantity in the system. Thus optical tomography allows measurement of spatially resolved parameters with the accuracy of integrated techniques.

Optical tomography has other advantages. Optical access is only required in the plane being imaged. This is important for systems such as jet engines and tokamaks, where imaging perpendicular to the region of interest is impossible. In addition, because each plane may be imaged indepen-

dently, many planes may be measured at the same time, allowing simultaneous acquisition of three-dimensional images.

Optical tomography has been demonstrated with both phase (6–12) and absorption (13–15) measurements. Phase measurements can give spatially resolved values of density in single-component fluid flows (6). In constant pressure systems, phase measurements can give information about temperature (7, 10) or composition (7). Absorption tomography can be used to measure both temperature and concentration variations, which is useful in combustion studies (15).

Tomography based on phase measurements has the advantage that the measurements may be made on any transparent flow, and no tunable laser is required. Tomography has been performed with phase measurements from beam deflection (6–8), interferometry (9, 10), and holography (11, 12). Because interferometric and holographic techniques involve fringe counting, there is ambiguity in the sign of phase change across a fringe and a limitation on the dynamic range. Beam-deflection techniques do not have phase-sign ambiguities and continue to be useful when large gradients would create too many fringes to resolve or when vibration could wash out fringes. Beam-deflection techniques can be very sensitive as well. We have demonstrated sensi-

tivity down to 35 nanoradians, which is equivalent to a change equal to 1/23,000 of an interference fringe over the laser-beam spot size (0.81 mm). As no reference beam is necessary for beam-deflection measurements, stability is required only on a single optical path.

Another significant advantage of beam-deflection measurements is that they can be applied to larger systems. If a system under investigation is proportionally scaled to a larger size, the beam deflections remain the same size. That is, although the path length scales up, the gradients scale down, and the net deflection remains the same. This is in contrast to fringe-counting techniques for which the number of fringes increases proportionally to the integration length and may reach an impractical number.

As a demonstration of the capabilities of beam-deflection optical tomography, we have performed measurements of density in a supersonic expansion of nitrogen gas from a nozzle. The variation of the equation of state in such an expansion is well understood (13) and provides a good check for our measurements. The flow is also very reproducible. We have examined supersonic expansions from single and multiple nozzles. For the single expansion measurements, a tapered nozzle with a half angle of 5.5° and a throat diameter of 0.84 mm was used.

We have measured beam deflections in a simple manner, using a helium-neon laser beam, an 80-mm focal length transform lens, and a position-sensitive (split-element) detector, as shown in Fig. 1. The laser beam is deflected on transversing the supersonic expansion because of the gradients in the index of refraction. The transform lens is positioned one focal length from the position-sensitive detector. For an ideal lens and small deflections, all rays incident on the lens at a given angle are linearly mapped to a unique position in the focal plane of the lens. Thus the position-sensitive detector can directly measure the beam-deflection angle. A second 60-mm focal length lens is used to focus the laser beam, and this improves the spatial resolution in the expansion. A projection, or single view, through the supersonic expansion is taken by scan-

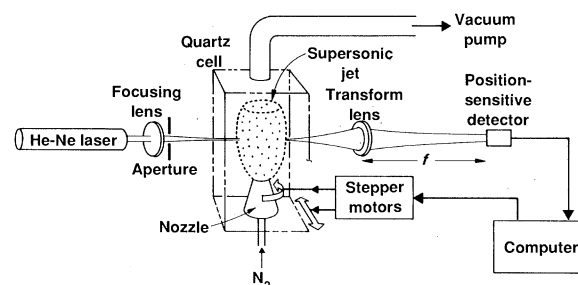


Fig. 1. Diagram of gas-flow, optical-imaging, and data-acquisition systems for beam-deflection optical tomography. The focal length of the transform lens (f) is 80 mm.

Edward L. Ginzton Laboratory of Physics, Stanford University, Stanford, CA 94305.

*Present address: Department of Physics/Atomic Physics, Lund Institute of Technology, Post Office Box 118, S-221 00 Lund, Sweden.

ning the nozzle through the laser beam with a stepper motor. A second stepper motor rotates the nozzle between projections to give multiple views. A total of 100 projections with 120 measurements per projection are taken for each reconstruction. The spatial resolution in the projections is $140\ \mu\text{m}$ horizontally and $50\ \mu\text{m}$ vertically. We obtained data and performed tomographic reconstruction with a Digital Equipment Corporation PDP-11/44 computer. We used a variation of the convolution back projection algorithm, modified to perform on beam-deflection projections (δ), to generate tomographic reconstructions. The convolution

back projection algorithm is based on a straight-line model and ignores the effects of refraction and diffraction. Applying such an algorithm to measurements made with optical plane waves without imaging optics can result in poor resolution (16). Because we used a focused beam as a probe, these effects were small. The largest beam-deflection angle in these measurements was 0.5 mrad, so beam crossing was not a problem.

Each reconstruction has 120 by 120 pixels on an 8 by 8 mm grid. The resulting reconstruction gives values of the real part of the index of refraction, n , which can be accurately related to the nitrogen density, ρ ,

through the law of Gladstone and Dale (17),

$$\rho = k(n - 1)$$
 where k is a constant.

By reconstructing a number of horizontal images at different heights and stacking them, we have been able to produce a three-dimensional image. Using a set of 13 images from equally spaced heights between 0.210 and 2.73 mm above the tapered nozzle, we have produced a three-dimensional image of the density in the supersonic expansion. A vertical section through this three-dimensional image is shown in Fig. 2a. The density drops very rapidly after the nitrogen gas exits the nozzle. There is more information in this image than can be shown in this reproduction. In an effort to show more detail, we have taken the logarithm of each pixel value in Fig. 2a to generate the image shown in Fig. 2b. As a result, the barrel shock surrounding the supersonic expansion is visible. The signal-to-noise ratio in Fig. 2b is quite good in spite of the logarithmic processing, which greatly reduces the dynamic range. This demonstrates the wide dynamic range in Fig. 2a, which is 500 to 1.

Horizontal sections through the three-dimensional image are shown in Fig. 3. The structure in the image of the barrel shock in Fig. 3, b and c, is real and not a reconstruction

Fig. 2. (a) Vertical section through three-dimensional reconstructed image of nitrogen density in a supersonic expansion. (b) Logarithm of the image in (a), showing the barrel shock. Each frame represents a height of 2.73 mm.

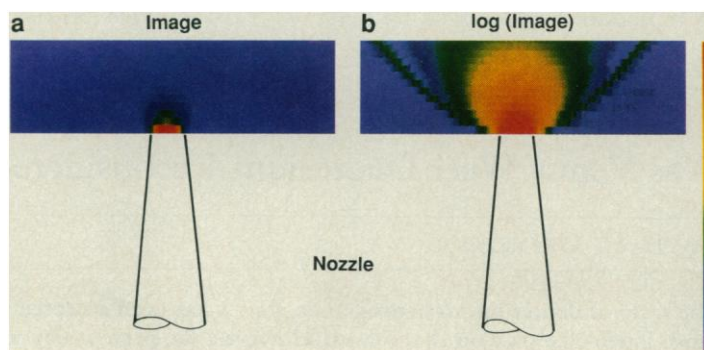
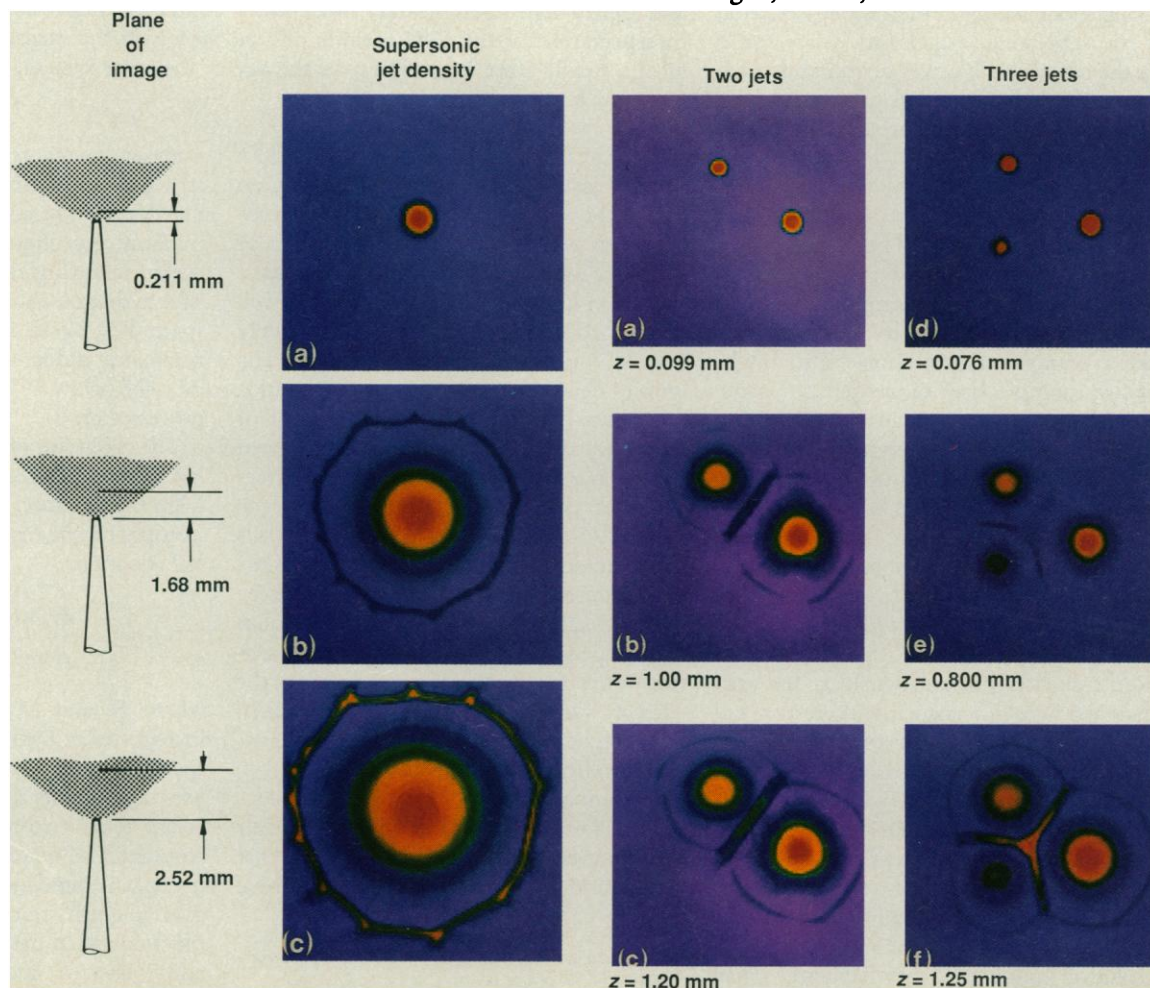


Fig. 3 (left). Horizontal sections through three-dimensional reconstructed image of nitrogen density in a supersonic expansion. The structure in the barrel shock is due to irregularities in the nozzle. Each frame represents a width of 8 mm. **Fig. 4 (right).** Horizontal images of the nitrogen gas density above two (a to c) and three (d to f) nozzles. Each frame represents a width of 8 mm. The height above the nozzle at which the image was generated is denoted by the variable z .



tion artifact. It is due to irregularities in the nozzle.

High-resolution images such as those in Figs. 2 and 3 contain interesting structural information about the flow. However, the images also contain accurate absolute information on the nitrogen density. The estimated root-mean-square error in the absolute density throughout the three-dimensional image of the jet is less than 3% of the peak value.

We also theoretically calculated the density in the supersonic expansion (13) by means of measured values of the plenum temperature and pressure, the nozzle diameter, and the height above the nozzle. Comparing the experimentally measured densities within the barrel shock with the theoretically calculated ones at a height of 2.10 mm above the nozzle yielded a root-mean-square difference of 1.8% of the maximum density at that height, which was 0.045 mg/cm³. There are no free parameters in the theoretical calculation. The theoretical and experimental densities are calculated entirely independently.

We have also produced images of multiple expansions. The density in horizontal planes above two and three nozzles are shown in Fig. 4, a to c and d to f, respectively. Here strong shock waves form at the intersection of the supersonic expansions. Also visible are the barrel shock waves surrounding each expansion. As for the single expansion, these images also contain accurate information on the density at every point.

Acquiring instantaneous two- or three-dimensional images with beam-deflection optical tomography would be advantageous. As the apparatus required for these measurements is very simple, multiple optical systems can be constructed to simultaneously take a number of projections. This might involve multiple laser diode-detector pairs, moiré deflectometry systems (8), or differential interferometry systems. Differential interferometers also measure gradients in the index of refraction and have some of the advantages described above for beam-deflection measurements. Other experiments (7-10, 12, 13, 15) have shown that good quality images may be produced with a small number of projections (ten or fewer). The technique that uses position-sensitive detectors described here is particularly interesting because both phase and absorption may be measured simultaneously. Combined phase-absorption tomography would be useful for concentration measurements in strongly refracting flows, for example. Considering the simplicity of the apparatus required for beam-deflection tomography and the accuracy, wide dynamic range, and high spatial resolution obtained, the technique may

prove valuable in a variety of fields of study ranging from turbulence to plasma instabilities.

REFERENCES AND NOTES

1. S. A. J. Druet and J. P. E. Taran, *Prog. Quantum Electron.* **7**, 1 (1981); R. J. Hall and A. C. Eckbreth, *Laser Appl.* **5**, 213 (1984).
2. G. Kychakoff, P. H. Paul, I. van Cruyningen, R. K. Hanson, *Appl. Opt.* **26**, 2498 (1987); G. Kychakoff *et al.*, *Science* **224**, 382 (1984).
3. B. Yip, D. C. Fourquette, M. B. Long, *Appl. Opt.* **25**, 3919 (1986).
4. B. Yip, J. K. Lam, M. B. Winter, M. Long, *Science* **235**, 1209 (1987).
5. S. R. Deans, *The Radon Transform and Some of Its Applications* (Wiley, New York, 1983).
6. G. W. Faris and R. L. Byer, *Opt. Lett.* **12**, 72 (1987).
7. ———, *ibid.*, p. 155 (1987).
8. J. Stricker, *Appl. Opt.* **23**, 3657 (1984).
9. R. Snyder and L. Hesselink, *ibid.* **24**, 4046 (1985).
10. H. M. Hertz, *Opt. Commun.* **54**, 131 (1985).
11. W. Alwang, L. Cavanaugh, R. Burr, A. Hauer, "Optical techniques for flow visualization and flow field measurements in aircraft turbomachinery," item 1, Final Report, Naval Air Systems Command contract N00019-69-C-0322, PWA-3942 (Pratt & Whitney Aircraft Company, East Hartford, CT, 1970).
12. R. D. Maltulka and D. J. Collins, *J. Appl. Phys.* **42**, 1109 (1971).
13. G. W. Faris and R. L. Byer, *Opt. Lett.* **11**, 413 (1986).
14. K. E. Bennett, G. W. Faris, R. L. Byer, *Appl. Opt.* **23**, 2678 (1984).
15. S. R. Ray and H. G. Semerjian, *Prog. Astronaut. Aeronaut.* **92**, 300 (1983).
16. A. J. Devaney, *IEEE Trans. Biomed. Eng.* **30**, 377 (1983).
17. F. J. Weinberg, *Optics of Flames* (Butterworth, London, 1963), p. 24.
18. We acknowledge the support of the U.S. Air Force Office of Scientific Research, Stanford University, and the Achievement Rewards for College Scientists Foundation.

17 July 1987; accepted 27 October 1987

Was Venus Wet? Deuterium Reconsidered

DAVID H. GRINSPON

The ratio of deuterium to hydrogen on Venus has been accepted as proof of a wetter, more Earth-like past on that planet. However, the present-day water abundance and the nonthermal hydrogen escape flux on Venus imply that hydrogen is in a steady state and that a hydrogen source, most likely cometary infall, is present. An alternative interpretation of the D/H ratio is offered, in which the measured value is consistent with a steady-state evolution over the age of the solar system. No past water excess is required to explain the isotopic data.

BOTTICELLI DEPICTED A WATERY birth of Venus, standing serenely on the shell of a giant clam. Planetologists have held a similar view of the birth of the love goddess' celestial counterpart. However, it may not have been so. It is well established that Venus is approximately 1×10^{-5} times as wet as Earth (1). The ratio of deuterium to hydrogen (D/H ratio) on Venus is 100 times as great as that of Earth (2, 3). This D/H ratio has been viewed as a residue from mass-selective fractionating escape of at least 100 times the current water abundance. According to this interpretation, the estimation of the primordial water endowment on Venus might be higher by an even greater factor if deuterium has escaped as well. An alternative explanation of the observed D/H ratio, based on the current water abundance and nonthermal hydrogen escape flux, requires only a steady-state evolution of water on Venus.

Evolutionary studies have typically concentrated on accounting for the loss of water on Venus because it has been assumed that Venus and Earth had similar primordial

water endowments (4). A consistent picture emerged, supported by detailed modeling, that Venus lost its endowment through a runaway greenhouse effect that boiled its oceans, allowing rapid photolysis of water. The hydrogen thus produced escaped into space, first by an extremely rapid hydrodynamic flux and later, when the water mixing ratio fell below 15%, by various nonthermal processes (5, 6).

The evolution of the D/H ratio on Venus has been presented as an example of Rayleigh fractionation (5). The escape of these isotopes can be represented by two differential equations

$$dH/dt = -KH \quad (1)$$

$$dD/dt = -KfD \quad (2)$$

where H and D represent the planetary inventories of hydrogen and deuterium, respectively, and f is the fractionation factor, which represents the efficiency of deuterium escape relative to hydrogen. The use of the constant K to represent the relation between hydrogen abundance and escape rate glosses over a much more complicated nonlinear function which has been derived by Kasting and Pollack (6) and Kumar *et al.* (5). How-

Lunar and Planetary Laboratory, University of Arizona, Tucson, AZ 85721.